Research Article

Binyamin Rubin*, Jason George and Riju Singhal

Effects of fixture rotation on coating uniformity for high-performance optical filter fabrication

https://doi.org/10.1515/aot-2017-0085
Received November 30, 2017; accepted February 15, 2018; previously published online March 15, 2018

Abstract: Coating uniformity is critical in fabricating high-performance optical filters by various vacuum deposition methods. Simple and planetary rotation systems with shadow masks are used to achieve the required uniformity [J. B. Oliver and D. Talbot, Appl. Optics 45, 13, 3097 (2006); O. Lyngnes, K. Kraus, A. Ode and T. Erguder, in 'Method for Designing Coating Thickness Uniformity Shadow Masks for Deposition Systems with a Planetary Fixture', 2014 Technical Conference Proceedings, Optical Coatings, August 13, 2014, DOI: http://dx.doi.org/10.14332/svc14.proc.1817.]. In this work, we discuss the effect of rotation pattern and speed on thickness uniformity in an ion beam sputter deposition system. Numerical modeling is used to determine statistical distribution of random thickness errors in coating layers. The relationship between thickness tolerance and production yield are simulated theoretically and demonstrated experimentally. Production yields for different optical filters produced in an ion beam deposition system with planetary rotation are presented. Single-wavelength and broadband optical monitoring systems were used for endpoint monitoring during filter deposition. Limitations of thickness tolerances that can be achieved in systems with planetary rotation are shown. Paths for improving production yield in an ion beam deposition system are described.

Keywords: bandpass filters; ion beam deposition; optical coatings; planetary rotation; uniformity.

***Corresponding author: Binyamin Rubin,** Veeco Instruments Inc., Advanced Deposition and Etch, Plainview, NY, USA, e-mail: brubin@veeco.com
Jason George and Riju Singhal: Veeco Instruments Inc., Advanced Deposition and Etch, Plainview, NY, USA

www.degruyter.com/aot

1 Introduction

Fabrication of optical interference coatings requires precise layer thickness control. Various open- and closed-loop endpoint control methods, including time power, quartz crystal monitoring, and optical monitoring [1], are used to ensure adequate thickness tolerance. In addition to precise control, good coating uniformity across substrate fixture is essential in enabling high throughput and yield of optical components.

Typical distribution of sputtered or evaporated material in a coating system is non-uniform. Different methods can be used to achieve uniform coating thickness, including different rotation patterns and shadow masking [2, 3]. It should be also noted that uniformity is affected by mechanical tolerances affecting substrate mounting, including offset, tilt, etc. [4].

Numerical modeling is widely used to simulate the distribution of sputtered material in order to optimize the deposition tool design and substrate fixturing. While distribution of sputtered material in thermal or e-beam evaporators can be modeled analytically [2], an ion beam sputtering plume is more complex and cannot be described by a simple cosine power law [5–8].

Coatings fabricated by ion beam sputtering (IBS) are used in high-end optical applications due to their superior properties that include low surface roughness, dense amorphous microstructure, and low optical losses [9, 10]. Some factors limiting more widespread application of IBS for optical coatings are film stress, lower deposition rates, and scalability challenges [11]. In recent years, progress was achieved in increasing deposition rate and throughput of IBS tools [12]. Planetary fixture with dual rotation allows increasing the total coating area with thickness uniformity on the order of a few percent. In order to further improve uniformity down to a fraction of a percent, shadow masking or varying deposition geometry, e.g. fixture plane tilt, is used.

In this work, we discuss the advantages and limitations of different fixture configurations. Numerical modeling is used to demonstrate how deposition geometry can be optimized for different fixture types. Experimental data demonstrating uniformity tuning for single and dual rotation fixtures are presented. The effect of fixture rotation on coating uniformity and random errors is analyzed, and the effect of these errors on coating yield is simulated numerically and confirmed in experiments.

2 Experimental system

Spector HT® and Spector 1.5® [12, www.veeco.com] dual IBS systems were utilized to deposit optical coatings discussed in this paper. The general layout of both systems is similar and is shown in Figure 1. Both systems employ a 16-cm ICP RF ion source to generate an ion beam that is made incident onto either a metal or dielectric target. These energetic ions sputter the target material, which then condenses onto a substrate. The source uses inductive coupling to ionize a working gas and a set of accelerating grids to which different electric potentials are applied. Electric potentials applied to the grids determine ion energy, and grid geometry determines spatial profile of the ion beam being extracted. Typically, beam energies of 1000–1500 eV were used for sputtering. A 12-cm ICP RF ion source of the same design directed at a substrate fixture is used to assist the deposition when it is necessary to improve the coating properties. Spector 1.5 is available with both single rotation and planetary fixtures; the results of uniformity tuning for both fixtures are presented in section 4. The Spector HT system is generally similar to Spector 1.5 but was designed for higher throughout and target utilization. The results of uniformity tuning for Spector HT with a planetary substrate fixture with four of 310-mm-diameter substrates are presented in section 4. The filter yield data presented in section 5 were also obtained with this configuration. Optical monitoring systems such as the broad band Quest® [1, 13] or single-wavelength Sirius® are used for layer end-point control. All devices and software are manufactured by Veeco Instruments, Inc.

3 Numerical modeling of coating uniformity

Numerical modeling of the distribution of sputtered material in an ion beam deposition tool was performed using MATLAB (The MathWorks, Inc.). As a first step, the ion

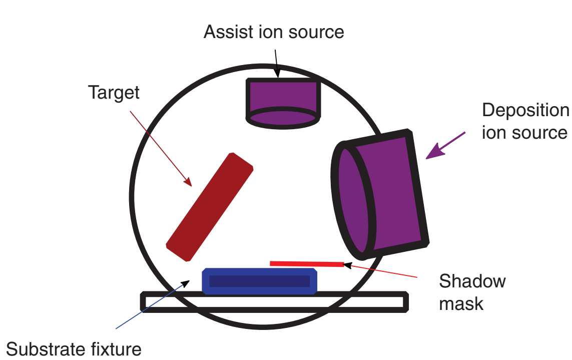

Figure 1: Spector 1.5/HT deposition geometry outline.

beam profile on a target was simulated. Using the known accelerating grid shape, positions of individual grid holes, and divergence of individual beamlets [14], integration is performed at each target point over individual beamlets:

$$J(x,y)=\sum_k \cos(\alpha)\frac{j_k(\gamma)}{r^2}, \tag{1}$$

where:

k = beamlet index
α = ion incidence angle at target surface
γ = angle relative to beamlet axis (Gaussian distribution of current density within beamlet was assumed)
r = distance between grid and target points

The resulting ion beam distribution was asymmetric and non-uniform as can be seen in Figure 2A.

The second step involved simulating the sputtering flux from the target. At this step, accurate representation of spatial distribution of sputtered material as a function of ion energy, incidence angle, ion, and target type is critical [7, 8]. This distribution is referred to as differential sputter yield in the literature [5, 6]. Although symmetric cosine power functions are often assumed and are predicted by some modeling, it was found experimentally that sputtering flux had an asymmetric distribution [5, 6]. Figure 2B shows the empirical differential sputter yield distribution measured using the experimental system described in Ref. [5] and used in the current work. In Figure 2, this distribution is represented by a colored hemisphere: the arrow shows the direction of incoming ions, and the color represents the amount of materials sputtered in different directions. The deposition plume is modeled by integrating ion beam distribution and differential sputter yield over the entire target area:

$$D(x_s,y_s)=\iint \frac{j(x_t,y_t)Y(\beta,\varphi,\theta)\cos(\delta)}{R^2}, \tag{2}$$

where:

x_s, y_s = substrate point coordinates
x_t, y_t = target point coordinates
Y = differential sputter yield
β = ion incidence angle
θ, φ = polar and azimuthal sputtering angles (see [5, 6])
δ = material arrival angle at substrate surface
R = distance between target and substrate points

A two-dimensional (2D) distribution of the sputtered material over the plane of the substrate, referred to as static deposition plume was determined (Figure 2C). To validate the model, a simulated static deposition plume

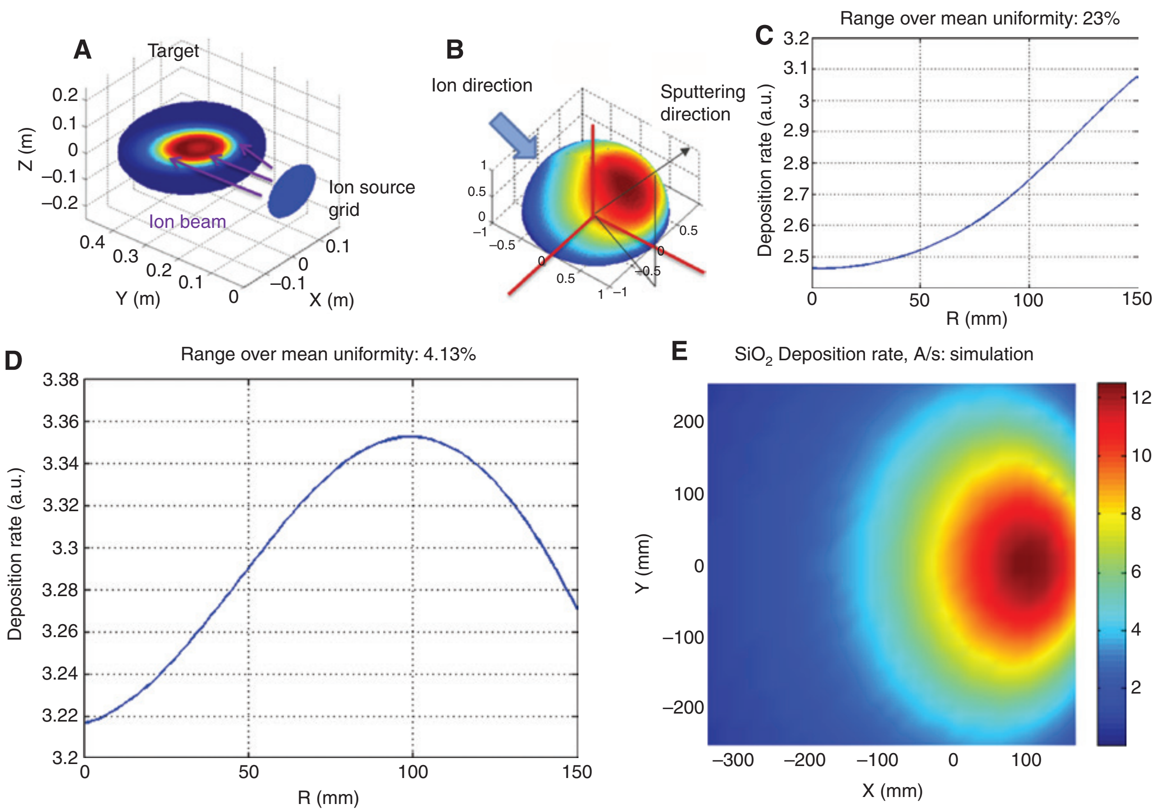

Figure 2: Simulations of ion beam current distribution and distribution of sputtered material.
Numerically simulated (A) ion beam distribution over a target surface from a 16-cm RF ion source. (B) Differential sputter yield. (C) The static deposition plume. (D) Comparison of SiO_2 deposition rates found by simulation and experimentally.

of SiO_2 was compared to the one experimentally measured (Figure 2D, E). While deposition profiles are similar, deposition rates are different by ~10%. This accuracy is adequate for studying the effects of coating uniformity, which is the main objective of the current work.

The last step involved calculating the coating distribution on the substrate taking into account the effects of fixture rotation. This was accomplished by integrating (averaging) the deposition rate along the trajectories of the different substrate points using known in-plane 2D distributions of deposition rate and known fixture kinematics. The trajectories of the substrate points were calculated using the following equations. For simple rotation

$$\begin{aligned} x &= R\cos(\omega t) \\ y &= R\sin(\omega t), \end{aligned} \tag{3}$$

where ω is the angular rotation speed, and t is the time. For planetary rotation

$$\begin{aligned} x &= R_s\cos(\omega t) + R_p\cos\left(\frac{N_s}{N_p}\omega t\right) \\ y &= R_s\sin(\omega t) + R_p\sin\left(\frac{N_s}{N_p}\omega t\right), \end{aligned} \tag{4}$$

where R_s is the distance from the planet center to the fixture center, R_p is the individual planet (substrate) radius, N_s and N_p are the number of teeth in the solar and planet gears.

The 2D interpolation was used to calculate the deposition rate along the substrate point trajectories using the static deposition plume data.

4 Uniformity optimization

4.1 Optimizing fixture position

Considering the deposition profile from Figure 2C, it can be expected that the deposition uniformity on a given substrate is defined by its position relative to the plume. We demonstrated this fact for the simple case of a planar substrate undergoing a single rotation about its center axis (a circular substrate/disc mounted on a single rotational axis fixture). Figure 3 shows that placing the center of rotation to the area of the maximum deposition rate leads to highly non-uniform radial distribution for a rotating substrate (Figure 3A), while the off-center

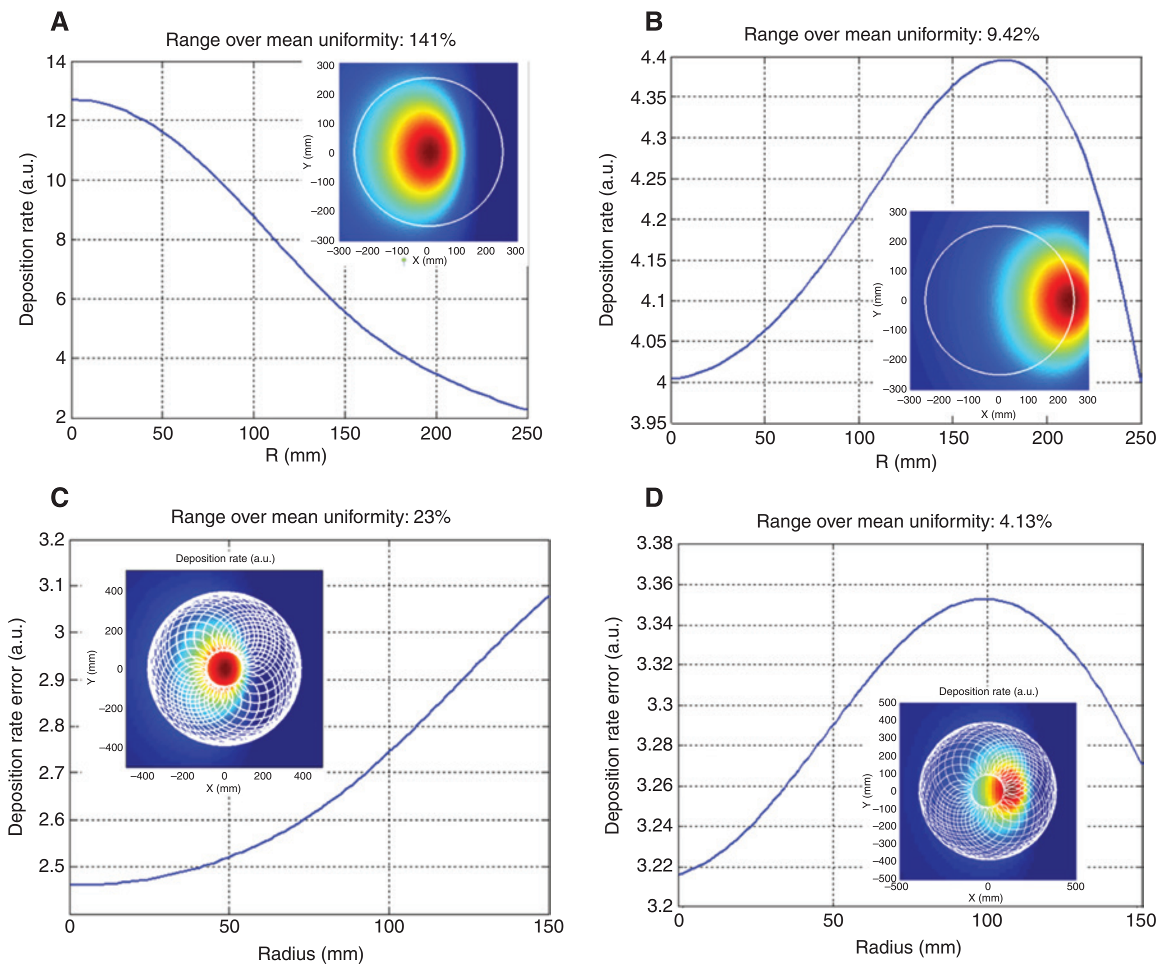

Figure 3: Radial deposition rate distributions for single and planetary rotation fixtures.
(A, B) Radial deposition rate profiles for single rotation fixture. (A) Deposition plume is centered with respect to the substrate (left inset) (B) Optimized off-center position of the substrate with respect to the deposition plume (right inset). (C, D) Radial deposition rate profiles for planetary fixture with centered (C) and optimized off-center (D) positions.

position can be optimized to achieve a significantly more uniform profile (Figure 3B). However, it may be noted that the off-center position underutilizes the deposition plume as a significant fraction of it misses contacting the substrate. Therefore, there is a trade-off between the deposition uniformity and throughput that needs to be considered when designing the deposition tool.

An alternate substrate arrangement for achieving better uniformity and higher throughput is to employ a planetary style (dual-axis) substrate rotation wherein substrates are mounted on multiple individual planets that rotate about their own axes and revolve about the center axis. This configuration allows achieving better coating uniformity on multiple substrates while increasing the utilization of the deposition plume. Inset in Figure 3C shows the trajectory of a point on the edge of a planet within the deposition plume. In contrast to Figure 3A where a point on the edge of a single rotational axis substrate retraces its circular trajectory with every rotation of the substrate, a complex hypo-cycloidal trajectory of the point on the planet typically has much longer repetition period. This path, shown in insets in Figure 3C and D, leads to more points on the planetary substrates accessing different regions of the deposition plume leading to a more uniform deposition profile. Proper selection of a number of teeth in the solar and planet gears is very important and is considered in detail in Refs. [2], [4], and [15]. Figure 3C and D also shows that as observed for simple rotation in Figure 3A and B, the radial uniformity in the case of a planetary fixture can be optimized by adjustment of its position toward the off-center from the deposition plume. The effects of the off-center plume positioning on material utilization efficiency are discussed in Ref. [2]. The conclusions from that work are also relevant for the IBD plumes.

4.2 Further uniformity improvement and tuning

To achieve the required spectral performance and yield of the optical coating, it is typically necessary to further improve the thickness uniformity on the substrates. The thickness uniformity requirements can vary from several percent to several hundredth of a percent depending on the coating type. Besides, the manufacturing tolerances cause slight variation in thickness distributions between coating tools of the same type that need to be compensated to meet the process specifications.

One way to improve the uniformity of the deposition thickness over substrates is by optimizing the angle between the fixture and the target. Changing the tilt angle of a substrate holder relative to the deposition plume alters the radial distribution of the deposition rates on the substrates. In Spector 1.5, the planetary fixture can be tilted to optimize uniformity. Empirical formula based on linear extrapolation is employed to calculate the consecutive tilt angles corresponding to a desired uniformity starting from a given deposition profile. Experimental data shown in Figure 4A demonstrate how tilt angle can be adjusted to improve the radial coating uniformity on the rotating substrate.

Another common way to improve the coating uniformity is by using shadow masking. The shadow mask design is extensively discussed in the literature [2, 3], and commercial software for mask calculation is available (www.tablemountainoptics.com/software.shtml). A shadow mask is designed to a shape that blocks excess flux in the substrate radial zones where the average deposition rate is high. The mask shape can be calculated per the required uniformity and the substrate geometry and fixture (single rotational axis, or planetary). Experimental examples of uniformity improvement with shadow masks are shown in Figure 4B and C. It can be observed that the uniformity for both substrate configurations was improved when a mask of suitable shape was introduced in front of the substrates.

4.3 Azimuthal uniformity

The above discussion considered radial thickness distribution on a rotating substrate. Azimuthal non-uniformity is typically small compared to radial and is often overlooked. However, for sensitive multi-layer optical coatings, azimuthal uniformity can be a critical factor in determining the yield even if the radial uniformity is good. This is because azimuthal uniformity contributes to in-substrate and substrate-to-substrate thickness errors. Azimuthal uniformity can generally be improved by increasing the number of substrate rotations per coating layer to ensure better averaging of the deposition rates in the circumferential direction [2, 16]. To analyze azimuthal errors, the deposition rates at multiple substrate points with different azimuthal and identical radial positions on the substrate were integrated over time. The same static plume profile was used for single rotation and planetary fixture. Outlines of both fixtures are shown overlayed on the static deposition plume with the individual substrate points used in simulation highlighted (Figure 5A, D).

The quasi-random errors due to azimuthal non-uniformity simulated for both fixtures are shown in Figure 5B and E. To illustrate the origin of the azimuthal errors, the coating thickness evolution for an individual point on both fixtures is shown in Figure 5C and F. Typical end-point control algorithm is based on an assumption of constant deposition rate and, hence, linear accumulation of thickness vs. time. This trend is shown as a straight line on Figure 5C and F. When the coating layer is terminated, the actual thickness can deviate from the linear trend producing thickness errors shown as a difference between the actual and assumed thickness evolution. For

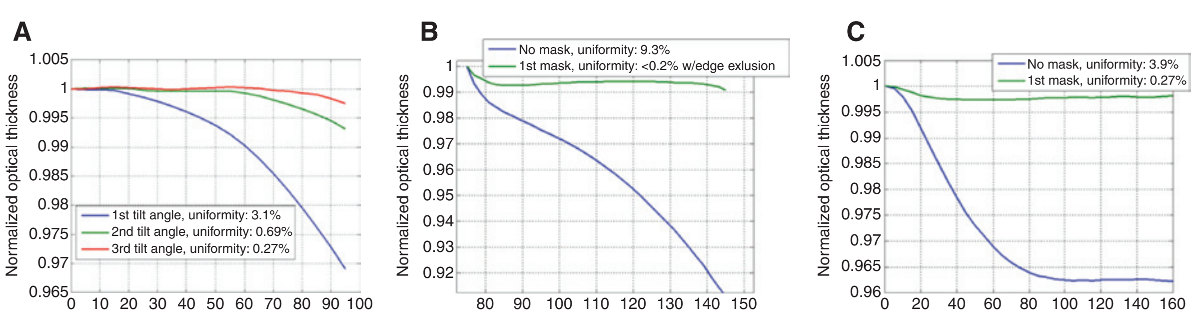

Figure 4: Experimental examples of radial uniformity improvement with fixture tilt adjustment and shadow masking. (A) Tilt angles of planetary fixtures were optimized to improve uniformity as observed with each successive tilt angle. (B) Mask design was calculated for single rotational axis fixture and (C) planetary fixture.

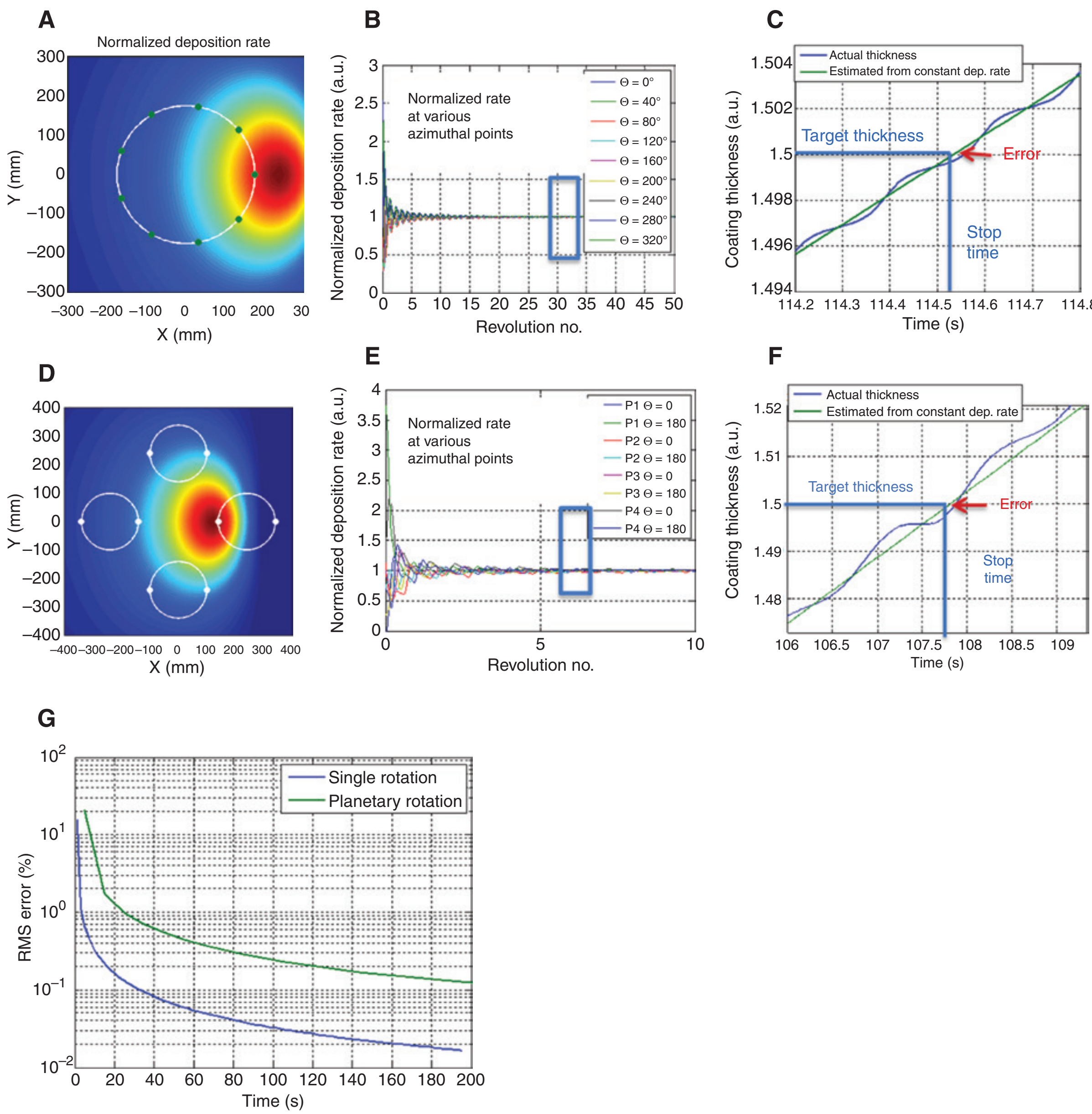

Figure 5: Static deposition plume with single rotation (A) and planetary (D) fixture outlines; locations of points used for azimuthal uniformity simulation indicated as dots.
Normalized deposition rate as a function of the number of fixture revolutions for single rotation (B) and planetary (F) fixtures. Deposition rate vs. time for typical conditions with (C) single rotation fixture, (F) planetary fixture. Evolution of RMS azimuthal thickness error with time for single rotation and planetary fixtures (G).

the single rotation fixture, the best averaging for all the points on the substrate is achieved at integer number of rotations; at these instances, the actual thickness evolution (Figure 5C, F) crosses the linear trend. For the planetary fixture, the best averaging at the integer number of rotations is achieved for centers of each planet only.

At any instance in the coating process, the thickness distribution at different points at a given substrate radius can be characterized by the RMS value. This RMS value, plotted in Figure 5G, for single rotation and planetary fixtures, reduces with coating time. In coating tools, including IBD, the single rotational axis fixture typically operates at high rotational speeds (~300 rpm) compared to a planetary fixture (~25 rpm). Assuming the deposition rates are comparable between single rotation and planetary fixture, the expected azimuthal errors are about an order of magnitude higher for a planetary fixture than a single rotation fixture. While uniformity on the order of

~0.25% can be achieved over a large area with planetary fixture, further uniformity improvement is limited by small azimuthal errors. This can be a limiting factor in producing certain types of sensitive coatings, which could be produced on the smaller-area single rotation fixtures.

5 Effect of non-uniformity and random errors on production yield

Based on the above results, we performed statistical modeling to estimate the production yields for two types of optical filters: a four-notch Vis-NIR fluorescence filter and a NIR narrow bandpass filter. Modeling was performed using the Optilayer (www.optilayer.com) software that uses the Monte-Carlo method to estimate the expected production yields. The production yields were estimated for a Spector HT IBS system with planetary fixture. The practical limit for the RMS radial uniformity that can be achieved with masking in this configuration is about 0.03%. Based on the above modeling results, the expected azimuthal RMS non-uniformity is about 0.04%, which results in an expected total RMS error of 0.05%. The yields of the two optical filters were analyzed: a broad four-notch fluorescence filter and a NIR narrow bandpass filter with a pass band of 2.5% of the center wavelengths. The filters were deposited in a Spector HT with planetary fixture that includes four substrates ('planets'). The actual production yields from the coating runs are compared to the modeling results in Table 1.

Table 1: Simulated and actual yields of two types of optical filters.

	Yield (modeling)	Yield (actual)
Four-notch filter	100%	100%
Narrow bandpass filter	45%	40%

A four-notch filter design comprised 100 layers with 21.4-μm total thickness. A broad band optical monitoring system (Quest®) was utilized for the layer endpoint control. The planetary fixture was preferred because of higher available coating area. A 100% production yield predicted by modeling was confirmed in experiments (Figure 6A), and therefore, using the planetary fixture was a successful strategy.

In a second experiment, a narrow bandpass filter design was coated. In this case, a single wavelength optical monitoring system (Sirius®) was utilized for the layer endpoint control. The single wavelength monitoring was used because of the required high spectral resolution and dynamic range considerations. The turning point control algorithm that provides error self-compensation was used [3]. The design had 98 layers and was 18 μm in overall thickness. A significant planet to planet variation in spectral position of the bandpass region can be observed in Figure 6B. In addition, the center wavelength and the spectral profile of the filter varied significantly within the substrate at the off-center substrate positions. This happened because not radial, but azimuthal, uniformity was the limiting factor, and the required uniformity could not be achieved with shadow masking. An experimental production yield of 40% was close to the theoretically predicted value of 45% that makes this strategy impractical.

An analysis of the narrow bandpass filter yield on the single rotation fixture was also performed theoretically. In this case, the azimuthal uniformity is much lower, and hence, radial uniformity that can be adjusted by masking

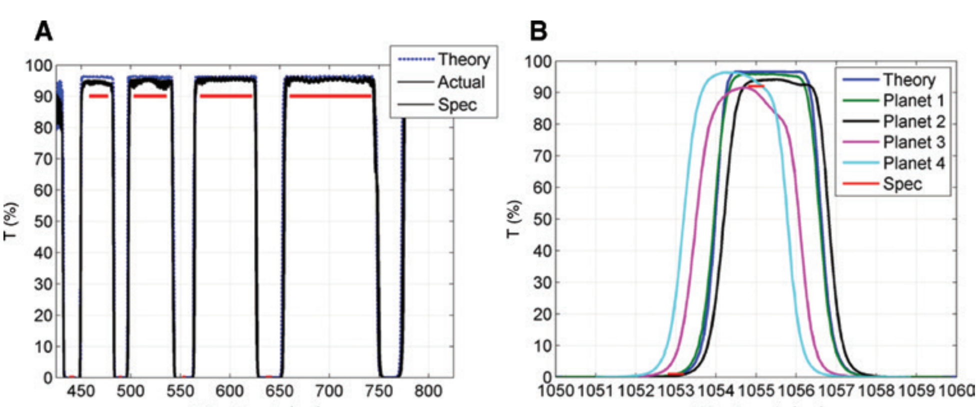

Figure 6: Optical transmission of filters deposited using planetary rotation fixture.
(A) Transmission spectrum of a four-notch filter. (B) Transmission spectrum of a narrow bandpass filter.

is a more significant factor. In this configuration, the expected RMS error value including the radial and azimuthal components is ~0.025%. The production yield predicted by the modeling is 85%. Based on these results, we developed a large-area single rotation fixture. It accommodates three of 200-mm wafers with a deposition rate higher than that of the planetary fixture. It is expected to provide high throughput while maintaining tight uniformity required for demanding applications such as narrow bandpass filters. Testing is under way; the results of the coatings fabricated with this fixture will be published in a later work.

6 Conclusion

There is a strong demand for highly advanced optical coatings for applications such as sensors, high-energy lasers, laser diodes, mirrors, etc. As each of these applications pushes the limits of state-of-the-art technology, there is a corresponding growing demand for equipment capable of manufacturing the building blocks of these devices with greater precision, repeatability, and cost effectiveness. Using some well-known optical coating designs as motivation, we first simulated the deposition plume within a Veeco Spector system. We consider two different types of substrate fixtures: the single rotational axis fixture and the planetary (dual rotational axis) fixture. It is shown with the help of numerical simulations that while higher throughput of less error-sensitive filters can be achieved with planetary fixture, the fabrication of highly sensitive narrow bandpass filters requires precision only achievable with the single rotation fixture. These modeling results were confirmed in an experiment. In order to achieve higher throughput with challenging coatings like a narrow band pass filter, new fixtures need to be designed and manufactured, which are currently being undertaken at Veeco Instruments, Inc.

Acknowledgments: We would like to thank Hector Castillo (Veeco Instruments, Inc.) for the help with the fabrication of the large-area single rotational axis fixture OGP measurements of the grids were not used in this work.

Author contributions: Binyamin Rubin performed all the simulations and experiments. Riju Singhal and Binyamin Rubin drafted the manuscript. Jason George supervised the entire work.

Competing interest: The authors declare no competing interest.

References

[1] D. Deakins, T. Ramin, B. Rubin and S. Chakmakjian, in 'Evaluation of Broadband Optical Monitoring for Optical Interference Coatings', 2014 Technical Conference Proceedings, Optical Coatings, August 21, 2014, DOI: http://dx.doi.org/10.14332/svc14.proc.1837.
[2] J. B. Oliver and D. Talbot, Appl. Optics 45, 13, 3097 (2006).
[3] O. Lyngnes, K. Kraus, A. Ode and T. Erguder, in 'Method for Designing Coating Thickness Uniformity Shadow Masks for Deposition Systems with a Planetary Fixture', 2014 Technical Conference Proceedings, Optical Coatings, August 13, 2014, DOI: http://dx.doi.org/10.14332/svc14.proc.1817.
[4] J. Oliver, Appl. Optics 55, 30, 8550 (2016).
[5] B. Rubin, J. Topper, C. Farnell and A. Yalin, Rev. Sci. Instrum. 80, 103506 (2009).
[6] B. Rubin, J. Topper and A. Yalin, J. Appl. Phys. D: Appl. Phys. 42, 205205 (2009).
[7] C. Bundesmann, T. Lautenschläger, D. Spemanna, A. Finzel, E. Thelander, et al., App. Surf. Sci. 421, Part B, 331 (2017).
[8] T. Lautenschläger, R. Feder, H. Neumann, C. Rice, M. Schubert, et al., Nucl. Instrum. Methods Phys. Res. B 385, 39 (2016).
[9] D. Wei, Appl. Optics 28, 14, 2813 (1989).
[10] J. R. Sites, P. Gilstrap and R. Rujkorakarn, Opt. Eng. 22, 4, 224447 (1983).
[11] R. Thielsch, A. Gatto and N. Kaiser, Appl. Optics 41, 16, 3211, (2002).
[12] J. Kraus, J. Davis, B. Rubin, O. Lyngnes and A. Ode, in 'Improving Throughput of Ion Beam Sputtered Optical Films', 2013 Technical Conference Proceedings, Optical Coatings, September 19, 2013, DOI: http://dx.doi.org/10.14332/svc13.proc.1086.
[13] O. Lyngnes, U. Brauneck, J. Wang, R. Erz, S. Kohli, et al., in 'Proc. SPIE 9627, Optical Systems Design 2015: Advances in Optical Thin Films V', 962715 (23 September 2015); doi: 10.1117/12.2194090.
[14] C. Farnell, 'Performance and lifetime simulation of ion thruster optics', Dissertation Thesis, 2007.
[15] J. B. Oliver, Appl. Opt. 56, 5, 1460 (2017).
[16] M. Gross, S. Dligatch and A. Chtanov, Appl. Opt. 50, 9, C316 (2011).

Binyamin Rubin
Veeco Instruments Inc., Advanced Deposition and Etch, Plainview, NY, USA, **brubin@veeco.com**

Binyamin Rubin obtained his PhD in Aerospace Engineering from Technion – Israel Institute of Technology and MSc and BSc from Moscow Institute of Physics and Technology. He has 10 years of experience developing ion thrusters for space propulsion and 6 years of experience developing ion beam deposition equipment for optical coatings.

Jason George
Veeco Instruments Inc., Advanced Deposition and Etch, Plainview, NY, USA

Jason George obtained his BS in Chemistry from the University of Florida and his MS in Mechanical Engineering from Colorado State University. Jason has over 17 years of optical coating and vacuum technology experience and has worked for Veeco for 16 years in various roles and responsibilities.

Riju Singhal
Veeco Instruments Inc., Advanced Deposition and Etch,
Plainview, NY, USA

Riju Singhal obtained his PhD in Materials Science and Engineering from Drexel University in 2012, and a B-Tech in Chemical Engineering from the Indian Institute of Technology, Kanpur in 2007. He has 5 years of experience in coating technologies including chemical vapor deposition and ion beam sputtering. He has been working with Veeco Instruments for the past 2.5 years in a technical product marketing role for the development of ion beam deposition equipment for optical coatings.